

# The Cause Analysis of the Incomplete Semi-Circle Observed in High Frequency Region of EIS Obtained from TEL-Covered Pure Copper

Qingli Cheng<sup>1,2</sup>, Zhuoyuan Chen<sup>1,\*</sup>

<sup>1</sup>National Engineering Research Center for Marine Corrosion Protection, Institute of Oceanology, Chinese Academy of Sciences, 7 Nanhai Road, Qingdao 266071, China

<sup>2</sup>University of Chinese Academy of Sciences, 19 (Jia) Yuquan Road, Beijing 100039, China

\*E-mail: [zychen@qdio.ac.cn](mailto:zychen@qdio.ac.cn)

Received: 11 April 2013 / Accepted: 9 May 2013 / Published: 1 June 2013

---

The occurrence of the incomplete capacitive semi-circle in the high frequency region of electrochemical impedance spectra was studied using thin electrolyte layer-covered two-electrode system. Thin electrolyte layer was made by evenly depositing NaCl particles onto the electrode surface and subsequently exposing to humid pure air with relative humidity of 84% and 25 °C. The incomplete capacitive semi-circle in the high frequency region was observed in low NaCl deposition density and in longer exposure duration of high NaCl deposition density. The occurrence of this incomplete capacitive semi-circle is decided by the nonuniformity of the current distribution on the electrode surface.

---

**Keywords:** Incomplete capacitive semi-circle, NaCl, Electrochemical impedance spectroscopy, Thin electrolyte layer, Copper

## 1. INTRODUCTION

Atmospheric corrosion is an electrochemical process occurred on a metal surface covered with a thin electrolyte layer (TEL) [1,2]. The corrosion processes under TEL, including the distributions of current and potential, the mass transport of oxygen, the hydration of dissolved metals and the accumulation of corrosion products, are greatly different from those in bulk solution. In case of TEL covered metal surface, the current and potential distribution is mainly controlled by resistance polarization. TEL thickness can decide the effective corrosion area on the TEL-covered metal surface [3].

During the past decades, there had been a lot of reports on the atmospheric corrosion behaviors of metals and their alloys under TEL [4-10]. Frankel *et al* [4] reported that the TEL thickness had a significant effect on the oxygen-limiting current density for the Type 304L stainless steel. Liao *et al* [5] presented that the limiting current density of dissolved oxygen increased with the decrease of TEL thickness in the range of 100-400  $\mu\text{m}$  for copper, whereas for AM60 magnesium alloys [6], cathodic reduction was inhibited with the decrease of TEL thickness.

Electrochemical impedance spectroscopy (EIS) is a very important technique for the investigation of the atmospheric corrosion of metals under TEL [7,11]. EIS can provide a non-destructive assessment of the atmospheric corrosion behaviors and can be used to study the corrosion mechanism. Since the perturbation of low amplitude is employed, the electrode surface conditions are not changed during the EIS measurement, which makes EIS be attributed to *in-situ* investigations. Meanwhile, the current passing through the working electrode and the counter electrode is very low because of low disturbance amplitude, which decreases the effect of resistance polarization under TEL. Nishikata *et al* [8] studied the atmospheric corrosion of Type 304 stainless steel covered with NaCl solution layer with the thickness of 10-1000  $\mu\text{m}$  using EIS. They found that the EIS data could be described by a transmission line model. The current distribution could be estimated from the Bode plots. If the phase angle went no further than  $-45^\circ$ , the current distribution was non-uniform at least in the low frequency region.

Although a large amount of work had been performed on the atmospheric corrosion of metals, key questions are still existed regarding the understanding of the fundamental processes that occurred under TEL. An incomplete semi-circle, corresponding to a capacitive behavior, was observed in the high frequency region of EIS of metallic samples covered with TEL. Zhang *et al* [12] found that a new semi-circle appeared in the high frequency region of EIS for iron. Huang *et al* [9] reported that the semi-circle existed in the high frequency region was produced by the oxide film under TEL. It is still not clear for the mechanism and further studies need to be performed for the cause analysis of the appearance of the high frequency capacitive semi-circle under TEL. In the present work, the effect of NaCl deposition density and exposure time in the high frequency capacitive semi-circle was studied using EIS. The cause of the occurrence of this semi-circle in high frequency region was analyzed in this paper. Pure copper was selected in this study not only because of its importance in microelectronic devices, circuit boards, and artistic, structural, and architectural applications, but also because much work based on its corrosion had been performed.

## 2. EXPERIMENTAL

A two-electrode configuration was used in this study and the schematic diagram of it was shown in Figure 1. Two identical pure copper plates were embedded about 100  $\mu\text{m}$  apart in parallel in epoxy resin. The exposed area of each copper plate for testing measures 10 mm  $\times$  2 mm. The electrode was wet polished with SiC paper to 3000 grit before being ultrasonically cleaned in analytical grade ethanol for 5 min. Before testing, the copper electrode was placed in a desiccator for 24 h. 280 and 560  $\mu\text{g}/\text{cm}^2$  NaCl particles were evenly deposited onto the electrode surface and the deposition method was

described in detail in a previous study [13]. The electrode was then exposed in a controlled pure humid air with relative humidity (RH) of 84% and 25 °C. The airflow rate of the pure humid air passing through the exposure chamber was 50 mL/min.

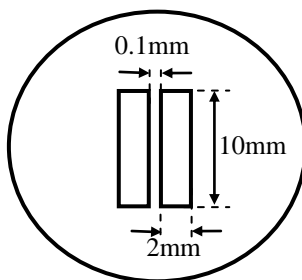


**Figure 1.** Schematic diagram of the two-electrode system used for the EIS measurements in this work.

The EIS measurements were performed using CHI 660D electrochemical workstation (Shanghai Chenhua Instrument Co., Ltd.). One of the copper plates was used as working electrode and the other one was used as both reference and counter electrodes. The EIS tests were done at open circuit potential over the frequency range between  $10^5$  and  $10^{-2}$  Hz, with an AC voltage magnitude of 10 mV, using 12 points/decade. The EIS measurements of this two-electrode system in 3.5% NaCl solution and 25 °C were performed for comparison.

### 3. RESULTS AND DISCUSSION

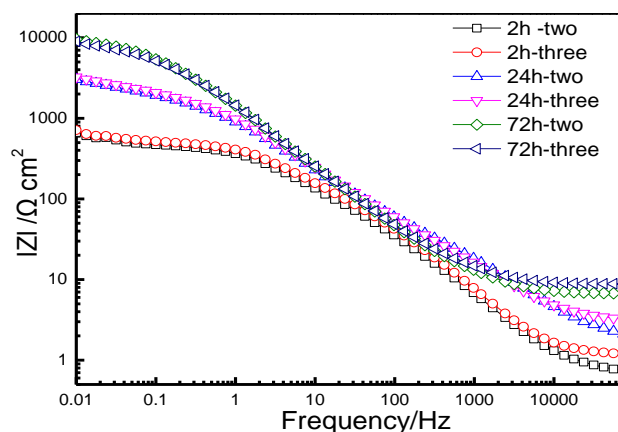


**Figure 2.** The EIS results of copper after 2, 24 and 72 h of exposure in 3.5% NaCl solution obtained using two-electrode system (Cu-Cu) and a standard three-electrode system (Cu-Pt-Ag/AgCl).

Two-electrode system was extensively used to perform the EIS measurements for the assessment of the corrosion behaviors of metals covered with TEL [8,14]. Using both a two-electrode system (Cu-Cu) and a standard three-electrode system (Cu-Pt-Ag/AgCl), EIS data were obtained in

3.5% NaCl solution for a comparative study for the suitability of two-electrode system in EIS measurements. Figure 2 shows the EIS results. The impedance values measured by two-electrode system are equal to those measured by standard three-electrode system in the entire frequency range, which reveals that two-electrode system can replace three-electrode system for the EIS measurements. Actually, this was also verified from previous reports [12,15].

In the present paper, a two-electrode system was employed for the EIS measurements of pure copper after deposited with 280, 560  $\mu\text{g}/\text{cm}^2$  NaCl particles and then after different exposure time (2, 24, 72h) in 84% RH and 25 °C. For comparison, EIS measurements were also performed in 3.5% NaCl solution using this two-electrode system. All of the EIS data are shown in Figures 3-5.

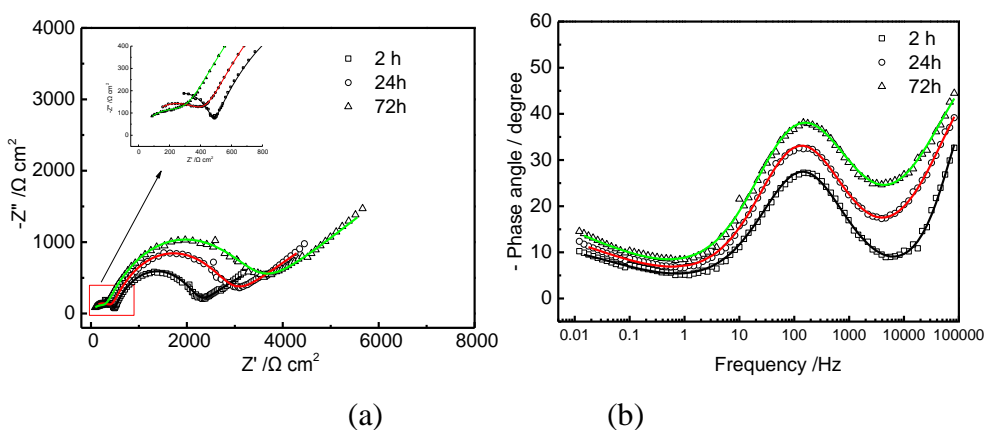


**Figure 3.** The Nyquist and Bode plots of copper deposited with 280  $\mu\text{g}/\text{cm}^2$  NaCl particles and then after different exposure time (2, 24, 72h) at 84% RH and 25 °C. (The dots with different symbols are the measured data and the solid lines are the fitting curves)

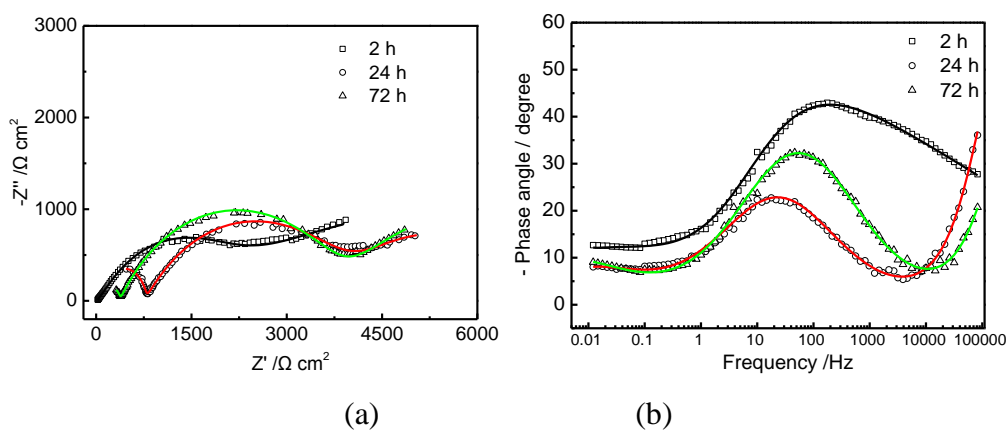


**Figure 4.** The Nyquist and Bode plots of copper deposited with 560  $\mu\text{g}/\text{cm}^2$  NaCl particles and then after different exposure time (2, 24, 72h) at 84% RH and 25 °C. (The dots with different symbols are the measured data and the solid lines are the fitting curves)

For the copper deposited with 280  $\mu\text{g}/\text{cm}^2$  NaCl particles, three time constants were observed after initial 2h of exposure, as the results showed in Figure 3. A time constant was observed in low frequency region, which is corresponded to charger transfer process of the corrosion reactions. Another

time constant was found at medium frequency, which is related to the corrosion product film. The third time constant was occurred at high frequency region, as confirmed by the Bode plots. An incomplete semi-circle in Nyquist plots, corresponding to a capacitive behavior, was exhibited in this frequency region. This time constant was existed in the entire exposure duration.

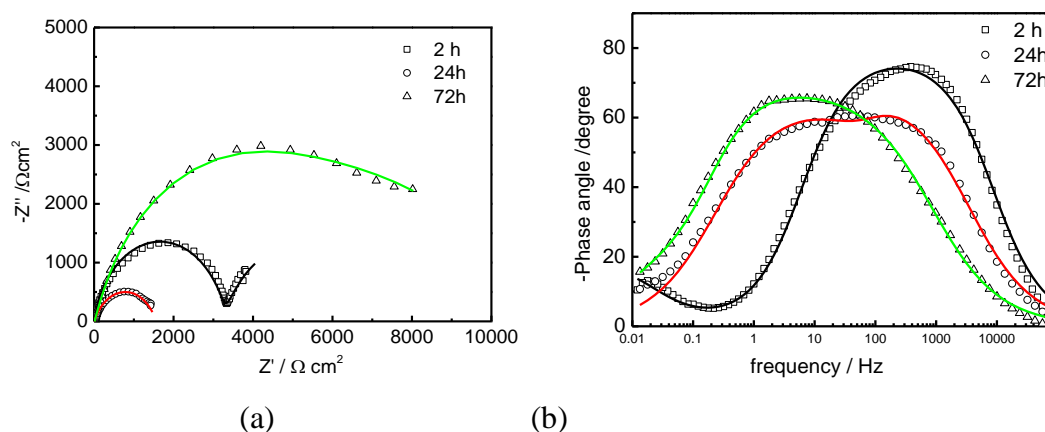


**Figure 5.** The The Nyquist and Bode plots of copper after different exposure time (2, 24, 72h) in 3.5% NaCl solution at 25 °C. (The dots with different symbols are the measured data and the solid lines are the fitting curves)

For the copper deposited with  $560 \mu\text{g}/\text{cm}^2$  NaCl particles, only two time constants were observed after initial 2h of exposure, as the results showed in Figure 4. This incomplete capacitive semi-circle was absent and the corresponding time constant disappeared in high frequency region after the initial 2h of exposure. However, with the increase of exposure time (24 and 72h), this time constant appeared again.

According to a previous work [3], a sample, deposited with NaCl particles, will absorb water from ambient environment and form a TEL on the sample surface if the RH is larger than the deliquescent point of NaCl particles, 75% RH. The NaCl concentration and the TEL thickness are decided by the RH, temperature and the NaCl deposition density if the particles are evenly distributed on the electrode surface. In the present work, 280 and  $560 \mu\text{g}/\text{cm}^2$  NaCl, which were evenly deposited on the electrode surface, would result in the formation of a TEL with the thickness of 12 and 24  $\mu\text{m}$  at 84% RH and 25 °C, respectively [3]. Corrosion during the initial 2h of exposure could be thought of as very slight. In this case, the corrosion of copper had quite little effect on the EIS spectra. Thus, it could be argued that the incomplete capacitive semi-circle at high frequency region was associated with the TEL thickness. When the TEL thickness was relatively thin, such as 12  $\mu\text{m}$ , this incomplete capacitive semi-circle appeared at high frequency region, however, when the TEL thickness increased to a certain value, such as 24  $\mu\text{m}$  in this work, this incomplete capacitive semi-circle was absent. In 3.5% NaCl solution, this incomplete capacitive semi-circle was not observed in the entire experimental exposure duration (Figure 5). The TEL thickness could be considered to be infinite at the condition of bulk solution.

As the results showed in Figure 4, the incomplete capacitive semi-circle at high frequency region appeared again after 24 and 72 h of exposure. According to a previous work [16], most of the chloride ions will be combined into the insoluble corrosion products with the increase of exposure time, such as  $\text{CuCl}$  and  $\text{Cu}_2(\text{OH})_3\text{Cl}$ , which make the TEL thickness decrease with the increase of exposure time. After 24 and 72 h of exposure, the TEL thickness decreased to a certain value and induced the occurrence of the incomplete capacitive semi-circle at high frequency region.

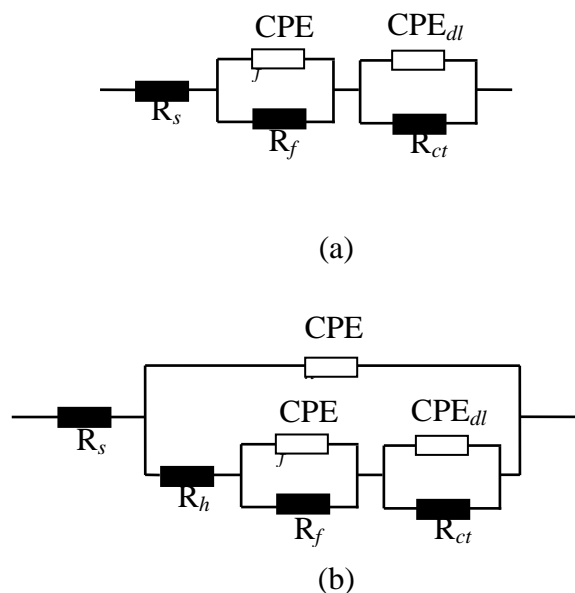


**Figure 6.** Equivalent circuits for fitting the EIS data obtained of pure copper with different NaCl deposition density and subsequently exposed at 84% RH and of pure copper exposed in 3.5% NaCl solution for 2, 24 and 72 h. (a) was used to fit the EIS spectra without the incomplete capacitive semi-circle at high frequency region and (b) was used to fit the EIS spectra with the incomplete capacitive semi-circle at high frequency region.  $R_s$  is the solution resistance;  $\text{CPE}_f$  and  $R_f$  are the capacitance and resistance of the corrosion product film formed during exposure, respectively.  $\text{CPE}_{dl}$  and  $R_{ct}$  are the double layer capacitance and the charge transfer resistance of the corrosion reactions, respectively.  $\text{CPE}_h$  and  $R_h$  are the capacitance and resistance corresponding to the incomplete capacitive semi-circle at high frequency region, respectively.

As the EIS data showed in Figure 3, the shapes of the EIS spectra haven't changed during the entire exposure duration (2-72 h), which indicate that the corrosion mechanism do not change significantly. The centers of the curvature of the incomplete capacitive semi-circles at high frequency region moved from the first quadrant to the fourth quadrant with the increase of exposure time, which revealed that the dispersion effect increased with exposure time. The dispersion effect is often caused by the geometrical inhomogeneity of the electrode surface or uneven current distribution on the electrode surface. All of the  $-\theta$  values in the Bode plots in Figure 3 are lower than  $45^\circ$ . Nishikata *et al* [8] reported that the uniformity of the current distribution on the electrode surface could be estimated from the Bode plot. The current distribution became uniform at least in the low frequency limit if the phase shift,  $\theta$ , went further than  $-45^\circ$  on the Bode plot. As showed in Figure 3, all of the phase angles

did not went further than  $-45^\circ$ , which indicated the uneven current distribution on the copper surface at this condition. However, at the initial exposure stage (2 h) of the electrode deposited with  $560 \mu\text{g}/\text{cm}^2$  NaCl, the phase shift,  $\theta$ , at the medium frequency region, went close to  $-45^\circ$ , indicating much more uniform current distribution in this case. The incomplete capacitive semi-circle at high frequency region was not observed at this condition. With the increase of exposure time, the phase angle went far away from  $-45^\circ$ , indicated that the current distribution became more and more uneven with the increase of exposure time. And, the incomplete capacitive semi-circle at high frequency region was observed again. As discussed above, the TEL thickness decreases with the increase of exposure time. The decrease of TEL thickness would result in the increase of resistance polarization, and hence, increased the non-uniform level of the current distribution. For bulk solution, all of the phase shifts,  $\theta$ , went further than  $-45^\circ$  on the Bode plot, which showed the uniform current distribution in this condition. The third time constant did not be observed on the Bode plots. Based on the above discussion, the uneven current distribution on the electrode surface resulted in the appearance of the incomplete capacitive semi-circle at high frequency region.

**Table 1.** Fitted parameters of the EIS of copper with different NaCl deposition densities and after 2, 24 and 72 h of exposure at 84% RH and 25 °C and in 3.5% NaCl bulk solution.

Fitted Parameters	280 $\mu\text{g}/\text{cm}^2$			560 $\mu\text{g}/\text{cm}^2$			3.5% bulk solution		
	2 h	24 h	72 h	2 h	24 h	72 h	2 h	24 h	72 h
$R_s (\Omega \text{ cm}^2)$	95.55	8.235	1.001E-7	6.008	72.06	81.24	5.712	1.439	8.499
$\text{CPE}_h (\mu\text{Fcm}^{-2} \text{ Hz}^{1-n_h})$	0.005581	0.2913	0.7472	-	0.002372	0.003109	-	-	-
$n_h$	0.9908	0.7167	0.6844	-	1	1	-	-	-
$R_h (\Omega \text{ cm}^2)$	375.9	418.9	315.7	-	703	289.1	-	-	-
$\text{CPE}_f (\mu\text{Fcm}^{-2} \text{ Hz}^{1-n_f})$	17520	10380	742.4	46.07	35.17	2511	12.61	449.2	607.8
$n_f$	0.3736	0.3188	0.3122	0.6523	0.6003	0.5485	0.8752	1	0.6476
$R_f (\Omega \text{ cm}^2)$	5624	32030	5.353E9	1749	3230	4091	3280	4.861	6445
$\text{CPE}_{dl} (\mu\text{F cm}^{-2} \text{ Hz}^{1-n_{dl}})$	7.993	6.915	7.134	682.2	2260	23.09	4931	488	207.4
$n_{dl}$	0.748	0.7567	0.7388	0.3294	0.5715	0.6329	0.7713	0.7291	0.8522
$R_{ct} (\Omega \text{ cm}^2)$	1664	2228	2744	7242	2850	3516	3782	1553	4460

According to the EIS data and the NaCl-induced atmospheric corrosion process of pure copper, two equivalent circuits, as shown in Figure 6, were established to fit the EIS results obtained at different conditions and after different exposure durations. Figure 6a was used to fit the EIS spectra without the incomplete capacitive semi-circle at high frequency region and Figure 6b was used to fit the EIS spectra with the incomplete capacitive semi-circle at high frequency region.  $R_s$  is the solution

resistance;  $CPE_f$  and  $R_f$  are the capacitance and resistance of the corrosion product film formed during exposure, respectively.  $CPE_{dl}$  and  $R_{ct}$  are the double layer capacitance and the charge transfer resistance of the corrosion reactions, respectively.  $CPE_h$  and  $R_h$  are the capacitance and resistance corresponding to the incomplete capacitive semi-circle at high frequency region, respectively.  $CPE_f$ ,  $CPE_{dl}$  and  $CPE_h$  are constant phase angle elements. Their impedance is equal to  $(Y_0(j\omega)^n)^{-1}$ , where  $\omega$  is the ac-voltage angular frequency (rad/s), and  $Y_0$  and  $n$  are the frequency-independent parameters. The  $n$  value represents a feature of dispersion effect in the Nyquist plot.

Figures 3-5 show both the experimental and the fitted results. The dots with different symbols are the measured data and the solid lines are the fitted curves. As showed in Figures 3-5, the given two equivalent circuits fitted the experimental results very well in most of the frequency range, which indicated that the given equivalent circuits were suitable for interpreting the initial NaCl-induced atmospheric corrosion behaviours of copper.

Table 1 shows the fitted parameters of the EIS of pure copper deposited with 280, 560  $\mu\text{g}/\text{cm}^2$  NaCl after different exposure durations at 84% RH and of pure copper in 3.5% NaCl solution. As the fitted parameters showed in Table 1, the  $n$  values for the incomplete capacitive semi-circle at high frequency region decreased with exposure time for copper deposited with 280  $\mu\text{g}/\text{cm}^2$  NaCl particles, which showed that the dispersion effect increased with exposure time. This is in agreement with that from the Nyquist plots showed in Figure 3, as in that the center of the curvature of the incomplete capacitive semi-circle at high frequency region moved from the first quadrant to the fourth quadrant with the increase of exposure time.

The values of the dispersion coefficient,  $n_f$ , of the phase angle element,  $CPE_f$ , are very small and they decrease with the increase of exposure time. This can be attributed to two main reasons. One is that more corrosion products are formed on the electrode surface with the increase of the exposure time, which roughen the electrode surface and hence make the dispersion effect increase. The other one is that the TEL thickness decreases with the exposure. The decrease of TEL thickness will increase the resistance polarization and hence increase the nonuniformity of the current distribution on the electrode surface, which increase the dispersion effect.

For the copper deposited with 560  $\mu\text{g}/\text{cm}^2$  NaCl, the dispersion coefficient has similar change trend with that of the copper deposited with 280  $\mu\text{g}/\text{cm}^2$  NaCl, indicating that the formation of the corrosion products and the decrease of the TEL thickness resulted in the increase of the dispersion effect. However, the values of  $n_f$  in this case are much higher than those of copper deposited with 280  $\mu\text{g}/\text{cm}^2$  NaCl, showed that the dispersion effect in this case is smaller than that of copper deposited with 280  $\mu\text{g}/\text{cm}^2$  NaCl.

For copper in 3.5% NaCl solution, the current distribution is uniform and the incomplete capacitive semi-circle in the high frequency region was not observed during the entire exposure. Hence, the appearance of the incomplete capacitive semi-circle in the high frequency region is associated with the nonuniformity of the current distribution on the electrode surface.

#### 4. CONCLUSIONS

In this work, the occurrence of the incomplete capacitive semi-circle in the high frequency region of EIS was studied using TEL-covered two-electrode system. TEL was made by evenly



depositing NaCl particles onto the electrode surface and subsequently exposed to humid pure air with 84% RH and 25 °C. For the copper deposited with 280  $\mu\text{g}/\text{cm}^2$  NaCl particles, this high frequency semi-circle was observed during the entire exposure duration. While, for the copper deposited with 560  $\mu\text{g}/\text{cm}^2$  NaCl particles, this high frequency semi-circle was absent at the initial 2 h of exposure. But, with the increase of the exposure time to 24 and 72 h, this high frequency semi-circle appeared again. For the copper electrode immersed into the 3.5% NaCl solution, this high frequency semi-circle was not observed in the entire exposure duration. The occurrence of the incomplete semi-circle in high frequency region was related to the TEL thickness viewed from the test results. However, it was decided by the nonuniformity of the current distribution on the electrode surface viewed from deep level of the corrosion mechanisms.

#### ACKNOWLEDGEMENTS

This work was financially supported by the Hundreds-Talent Program of the Chinese Academy of Sciences (Y02616101L).

#### References

1. K. Nassau, A. Miller, T. Graedel, *Corros. Sci.*, 27 (1987) 703.
2. C. Arroyave, M. Morcillo, *Corros. Sci.*, 37 (1995) 293.
3. Z. Y. Chen, F. Cui, R. G. Kelly, *J. Electrochem. Soc.*, 155 (2008) C360.
4. G. Frankel, M. Stratmann, M. Rohwerder, A. Michalik, B. Maier, J. Dora, M. Wicinski, *Corros. Sci.*, 49 (2007) 2021.
5. X. Liao, F. Cao, L. Zheng, W. Liu, A. Chen, J. Zhang, C. Cao, *Corros. Sci.*, 53(2011)3289.
6. W. Liu, F. Cao, A. Chen, L. Chang, J. Zhang, C. Cao, *Corros. Sci.*, 52 (2010) 627.
7. G.A. El-Mahdy, A. Nishikata, T. Tsuru, *Corros. Sci.*, 42 (2000) 1509.
8. A. Nishikata, Y. Ichihara, T. Tsuru, *Corros. Sci.*, 37 (1995) 897.
9. H. Huang, Z. Dong, Z. Chen, X. Guo, *Corros. Sci.*, 53 (2011) 1230.
10. M. Stratmann, H. Streckel, *Corros. Sci.*, 30 (1990) 697.
11. E. Dubuisson, P. Lavie, F. Dalard, J.P. Caire, S. Szunerits, *Corros. Sci.*, 49 (2007) 910.
12. S. Zhang, S. Lyon, *Corros. Sci.*, 36 (1994) 1309.
13. Z.Y. Chen, S. Zakipour, D. Persson, C. Leygraf, *Corrosion*, 60 (2004) 479.
14. A. Nishikata, Y. Ichihara, Y. Hayashi, T. Tsuru, *J. Electrochem. Soc.*, 144 (1997) 1244.
15. X. Zhang, W. He, I. Odnevall Wallinder, J. Pan, C. Leygraf, *Corros. Sci.*, 44 (2002) 2131.
16. Z. Y. Chen, D. Persson, A. Nazarov, S. Zakipour, D. Thierry, C. Leygraf, *J. Electrochem. Soc.*, 152 (2005) B342.